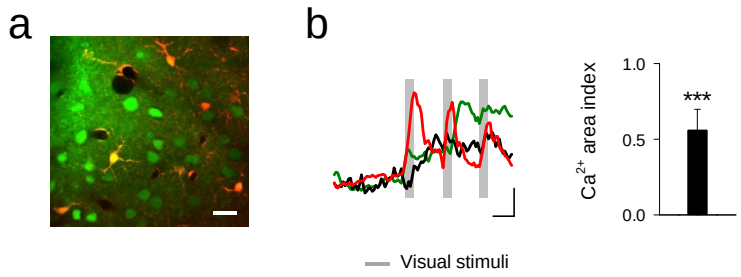


**Supplementary Figure 1. Astrocyte visual responses in V1.** (**a**) Representative double labeling image of astrocyte marker SR101 (red) and cells bulk-loaded with OGB (green) in V1 (120 µm below the pial surface; scale bar, 40 µm). (**b**) Astrocyte calcium visual responses in V1. Gray vertical bars indicate time segments when visual stimuli were presented (cf.[8]). Population average of $Ca^{2+}$ area index induced by visual stimulation (n = 22 astrocytes from 2 mice). Visual stimuli (gray vertical bars) were presented for 8 s. Scale bar 20%, 20 s. *** $P < 0.001$, Wilconox test. Error bars indicate SEM.

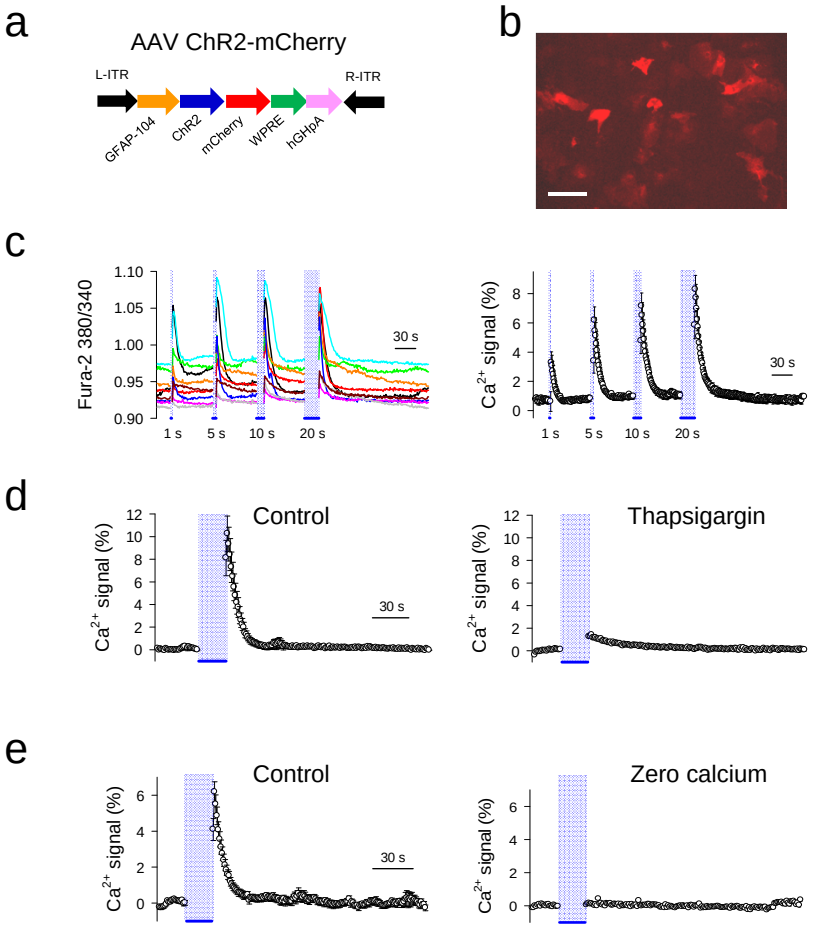


**Supplementary Figure 2. ChR2 evokes reliable calcium elevations in cultured astrocytes**. (**a**) Schematic for the viral vector used for astrocyte-specific expression of ChR2 (AVVs-GFAP104-ChR2-mCherry). (**b**) Fluorescence image of primary astrocyte culture cells expressing ChR2-mCherry. Scale bar, 60 μm. (**c**) Calcium elevations evoked by different durations of stimuli (1, 5, 10, 20 s @ 20 Hz; blue vertical bar; n = 9 astrocytes), and normalized calcium population average (*right*) evoked by these different stimuli (n = 15 astrocytes). Note the increase in the response to longer stimuli. (d) Calcium signals evoked by ChR2 stimulation in control (n = 20 astrocytes) and after incubation with Thapsigargin (1 μM; n = 48 astrocytes; 10 s @ 20 Hz; blue horizontal bar). (e) Calcium signals evoked by ChR2 stimulation in control medium and after replacing the incubation medium with zero calcium solution (n = 56 astrocytes; 20 s @ 20 Hz; blue horizontal bar). Note the contribution of intracellular calcium stores and extracellular calcium to the calcium responses evoked by ChR2 stimulation (cf.[14,23]). Error bars indicate SEM.

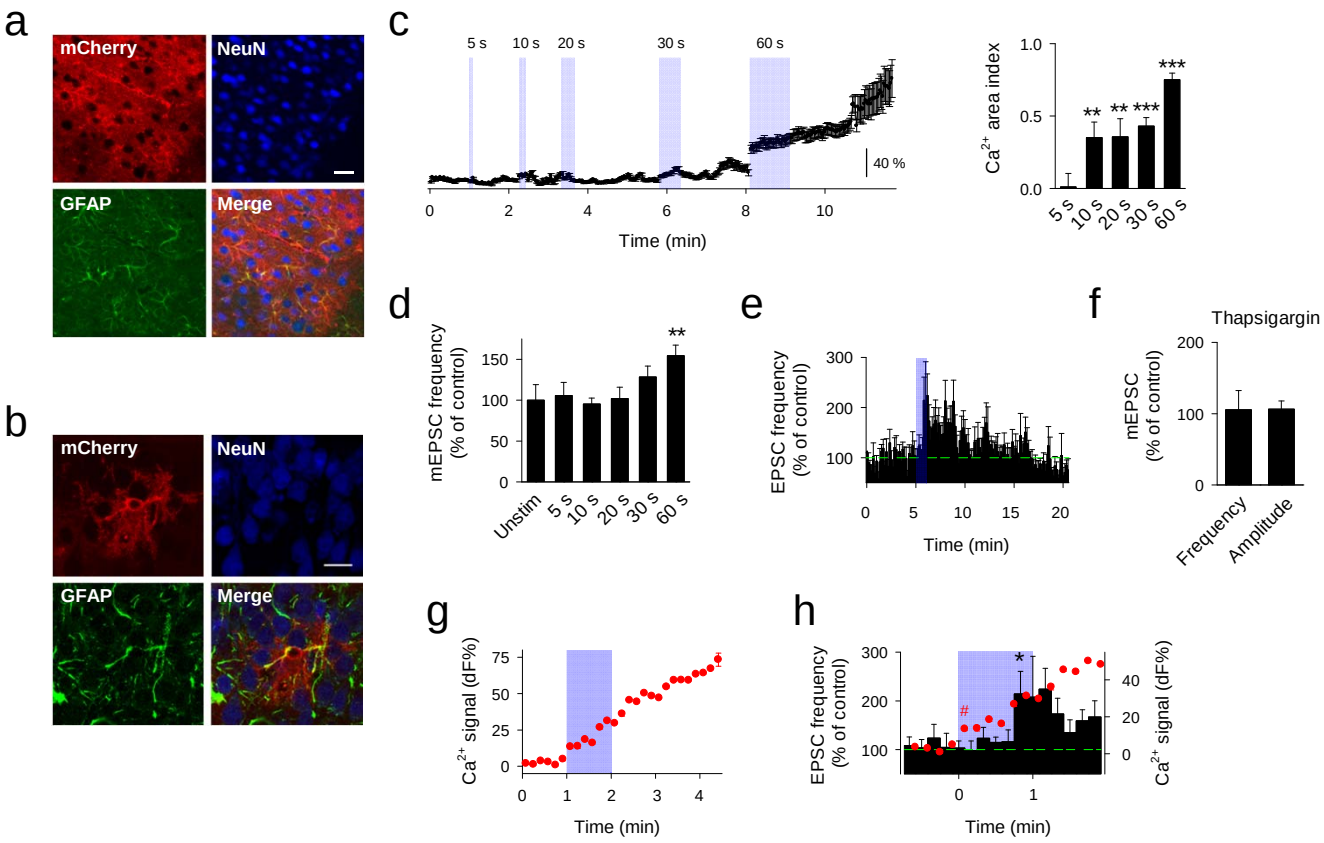


**Supplementary Figure 3. ChR2 stimulus duration vs calcium elevations and mEPSC responses relationship in V1 slices.** (**a**) Representative images of immunocytochemical localization of ChR2-mCherry, NeuN and GFAP in V1 cortical slices in C57/BL6 mice transfected with AAV2.5-GFAP-ChR2–mCherry (n = 3 mice). Note the selective expression of ChR2-mCherry in astrocytes *(bottom).* Scale bar, 60 μm. (**b**) Detail of an mCherry labeled cell showing the specific colocalization with GFAP staining but the absence of colabeling with NeuN staining, indicating the selective expression of ChR2-mCherry in astrocytes but no in neurons. Scale bar, 20 μm. (**c**) (*Left*) Time course of astrocyte $Ca^{2+}$ signals due to ChR2 stimulation of 5, 10, 20, 30, 60 s duration (blue vertical bar) at 20 Hz,. (*Right*) $Ca^{2+}$ area index at different durations (n = 59 astrocytes). **P < 0.01, *** P < 0.001; Wilconox test. (**d**) Relative changes of mEPSC frequency and amplitude in the basal conditions (unstim) and after 5, 10, 20, 30, 60 s duration at 20 Hz of ChR2 stimulation (n = 9 neurons). **P < 0.01, t-test. Note that ChR2 stimulation evoked changes in $Ca^{2+}$ area index at 10 s duration but synaptic transmission was significantly affected by longer duration of stimulation (60 s). (**e,g,h**) Time course of ChR2-induced changes in EPSCs. (**e**) Histogram of relative change of spontaneous EPSC frequency versus time (bin width 10 s) before and after astrocyte stimulation (20 Hz, 60 s; blue vertical bar; n = 9). Green dash line indicates reference baseline. (**f**) Relative changes of mEPSC frequency and amplitude baseline from control values after incubation with thapsigargin (1 μM) (n = 6). Thapsigargin did not significantly affect the basal levels of synaptic transmission but abolished astrocyte calcium signals and astrocyte-induced synaptic modulation (see Fig. 2d). (**g**) Astrocyte calcium signal induced by ChR2 stimulation versus time (bin with 10s; ChR2 stimulation blue horizontal bar; n = 76 astrocytes from n = 10 slices) (**h**) Superimposed astrocyte calcium signal (red dots) on EPSC histogram inset (black bars) showing the temporal course of both responses. Zero time corresponds to the beginning of ChR2 stimulation. Note that significant changes in astrocyte $Ca^{2+}$ signal preceded significant increases in EPSC frequency. The first data point with statistical difference for each parameter is shown. * P < 0.05 (in black, for EPSC). # P < 0.001 (in red, for $Ca^{2+}$ signal), t-test. Error bars indicate SEM.

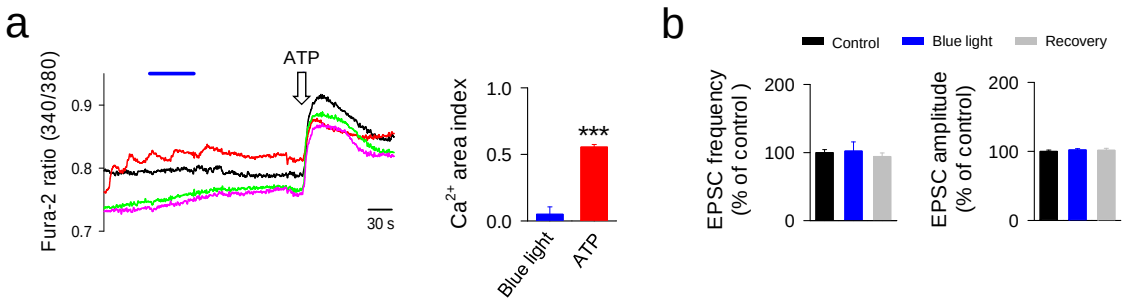


**Supplementary Figure 4. Blue light effects on naïve V1 slices.** (**a**) *Left,* Representative astrocytic calcium signals evoked by blue light (60 s @ 20 Hz), and ATP stimulation (20 mM, 1 s puff) in naïve astrocytes from uninfected contralateral V1 slices (no-ChR2 expression). Note that light stimulation failed to increase calcium levels in naïve astrocytes; however, ATP stimulation evoked calcium elevations in the same astrocytes, confirming the ability of these cells to increase their calcium excitability. *Right*, $Ca^{2+}$ area index by blue light and ATP (n = 22 astrocytes from 4 slices from 2 mice). ***P < 0.001; Wilconox test. (**b**) Relative changes in spontaneous EPSC frequency and amplitude in the basal conditions, induced by light stimulation and up to 10 min post stimulation (recovery) (n = 10 neurons). Error bars indicate SEM.

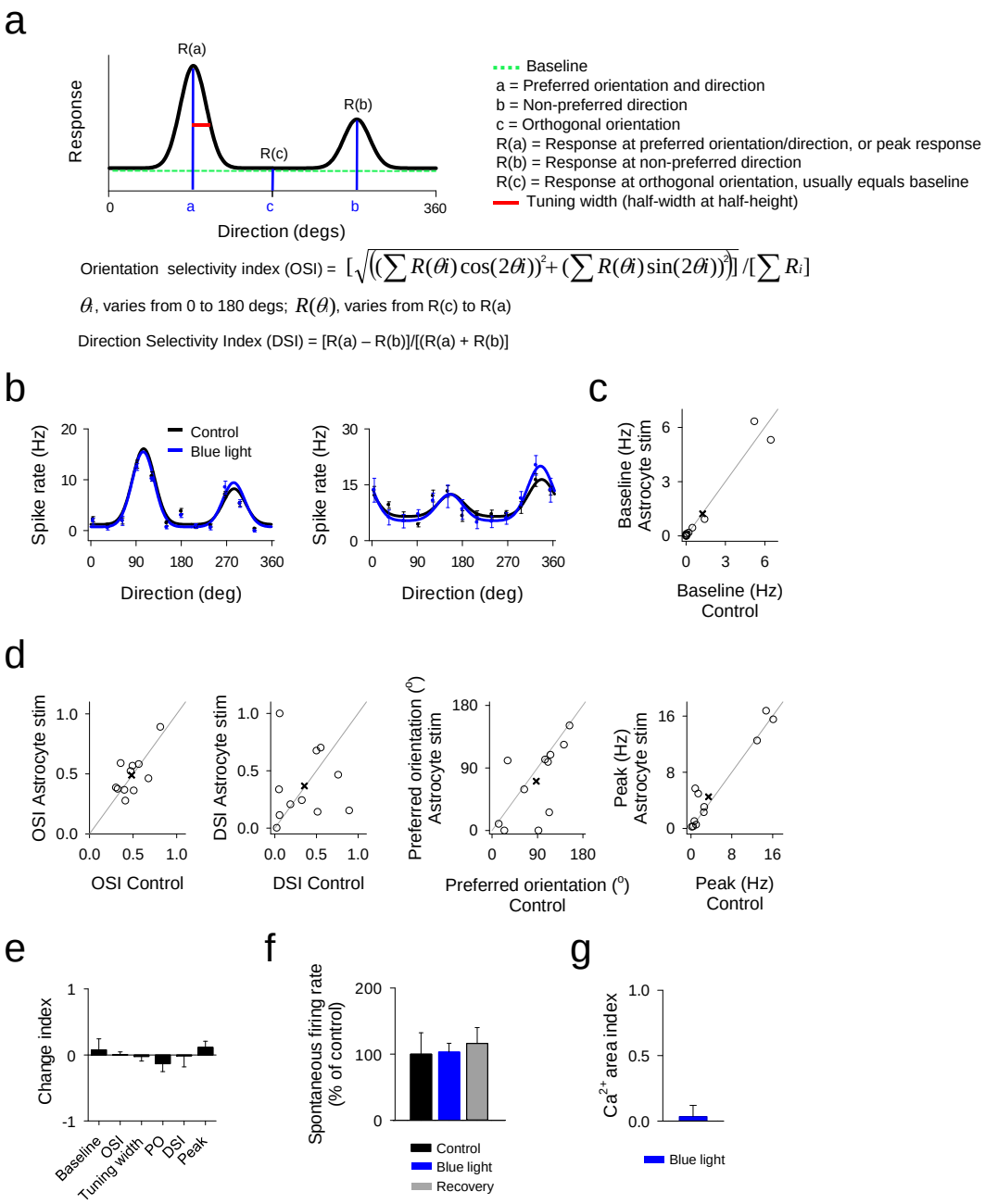


**Supplementary Figure 5. Effect of blue light on neuronal activity *in vivo* in mice with no GFAP-ChR2 transfection.** (**a**) Analysis of tuning curves. Schematic illustration of the orientation/direction tuning curve and its parameters, and calculation of the orientation and direction selectivity index. (**b**) Representative tuning curves of one putative excitatory-regular spiking cell (right) and fast spiking inhibitory cell (left) before (Control, black) and after blue light stimulation (blue) recorded by blind cell-attached recordings in non-transfected wildtype mice. Dots denote measured firing rates and lines denote fitted curves (n = 10 trials). (**c**) Population summary of astrocyte-induced changes in baseline firing rate (circle, individual cell; cross, population average; n = 11 from 4 mice). (**d**) Population summary of astrocyte-induced changes in OSI, DSI, preferred orientation, and peak firing rate (n = 11). (**e**) Index of change in tuning properties before and after astrocyte stimulation. (**f**) Relative changes of spontaneous firing rate (without visual stimuli) before (control), after light stimulation and 10 min post stimulation (recovery) (n = 11). Error bars indicate SEM. (**g**) $Ca^{2+}$ area index following blue light stimulation (n = 31 astrocytes from 2 mice). Error bars indicate SEM.

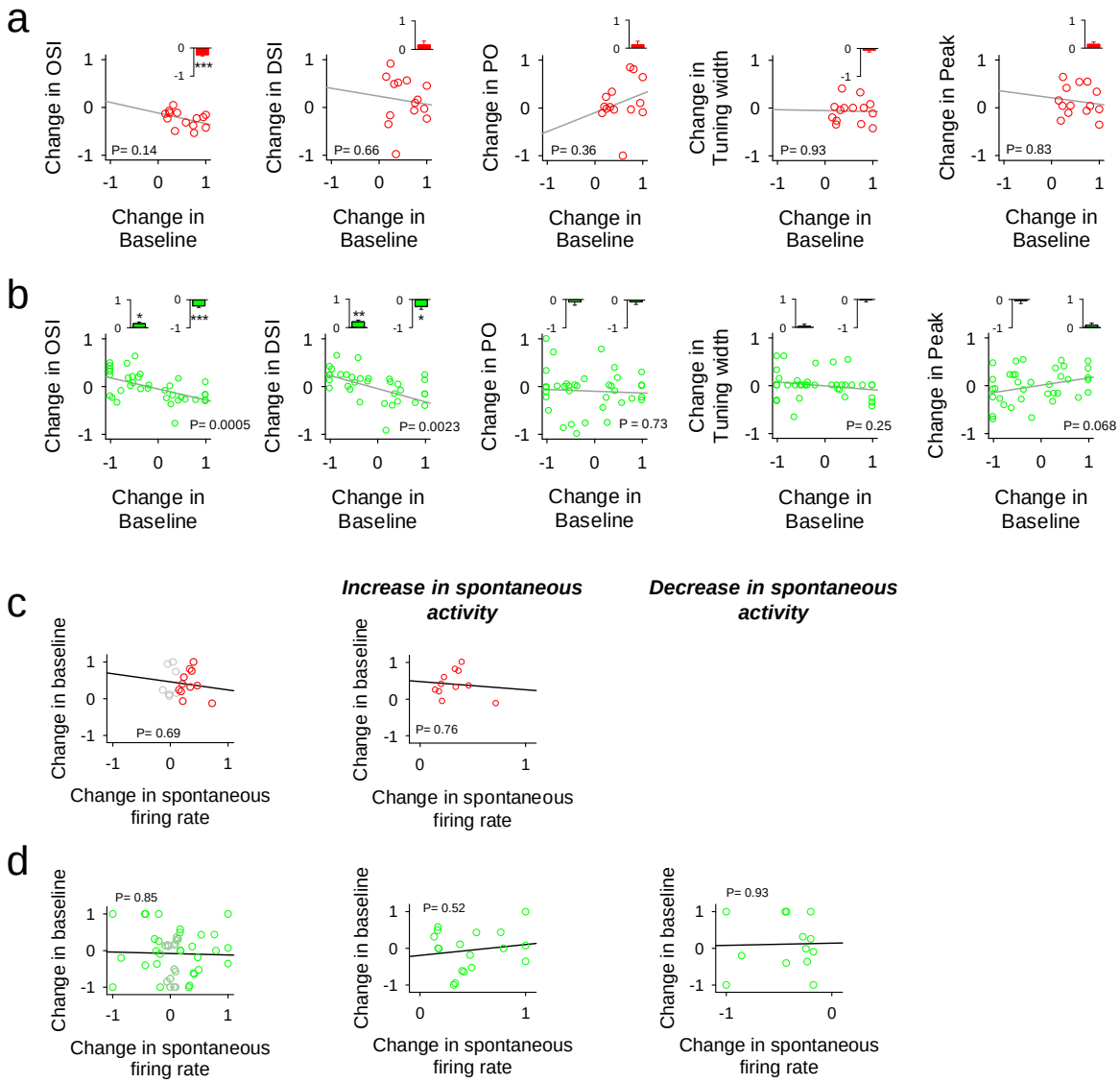


**Supplementary Figure 6. Astrocyte-induced changes in tuning parameters of excitatory cells and PV⁺ neurons.** (**a**, **b**) Normalized index of tuning parameters showing changes in OSI, DSI, preferred orientation, tuning width and peak amplitude vs baseline for PV⁺ neurons (**a**) and excitatory neurons (**b**). *Inset*: Normalized index for each parameter showing the population differences before and after astrocyte stimulation (from Fig. 6e and Fig 7e,g**)**. *Inset Left*, normalized index for cells that showed decreases in the baseline after astrocyte stimulation. *Inset Right*, normalized index for cells that showed increases in the baseline after astrocyte stimulation. Circle, individual cell. Dashed line, linear regression for the population. *P < 0.05, **P < 0.01, ***P < 0.001; Wilconox test. Error bars indicate SEM. These data show the impact of baseline changes on the feature-selectivity of visual responses (see text for details). For PV⁺ neurons, the baseline showed an increase and the population OSI showed a significant reduction after astrocyte photostimulation (inset in **a**, top left). Excitatory cells showed both an increase and decrease in the baseline; there was a significant negative correlation between changes in baseline and OSI and DSI, and the population OSI and DSI showed significant changes that were inversely related to the baseline changes (insets in **b**). (**c, d**) Changes in spontaneous firing rate vs changes in visual-evoked firing rate for PV⁺ neurons and excitatory neurons**.** (**c, d**) *Left,* Normalized index of firing rate showing changes in spontaneous firing rate vs baseline (visual-evoked firing rate) for PV⁺ neurons (**c**; n = 18 from 12 mice), excitatory neurons (**d**; n = 45 from 25 mice). *Center-right,* Cells were classified according to significant changes in spontaneous firing rate, and are shown in these panels under *Increase in spontaneous activity* and *Decrease in spontaneous activity.* Circle, individual cell. Dashed line, linear regression for the population. Grey circles denote cells with no significant changes in spontaneous firing rate.

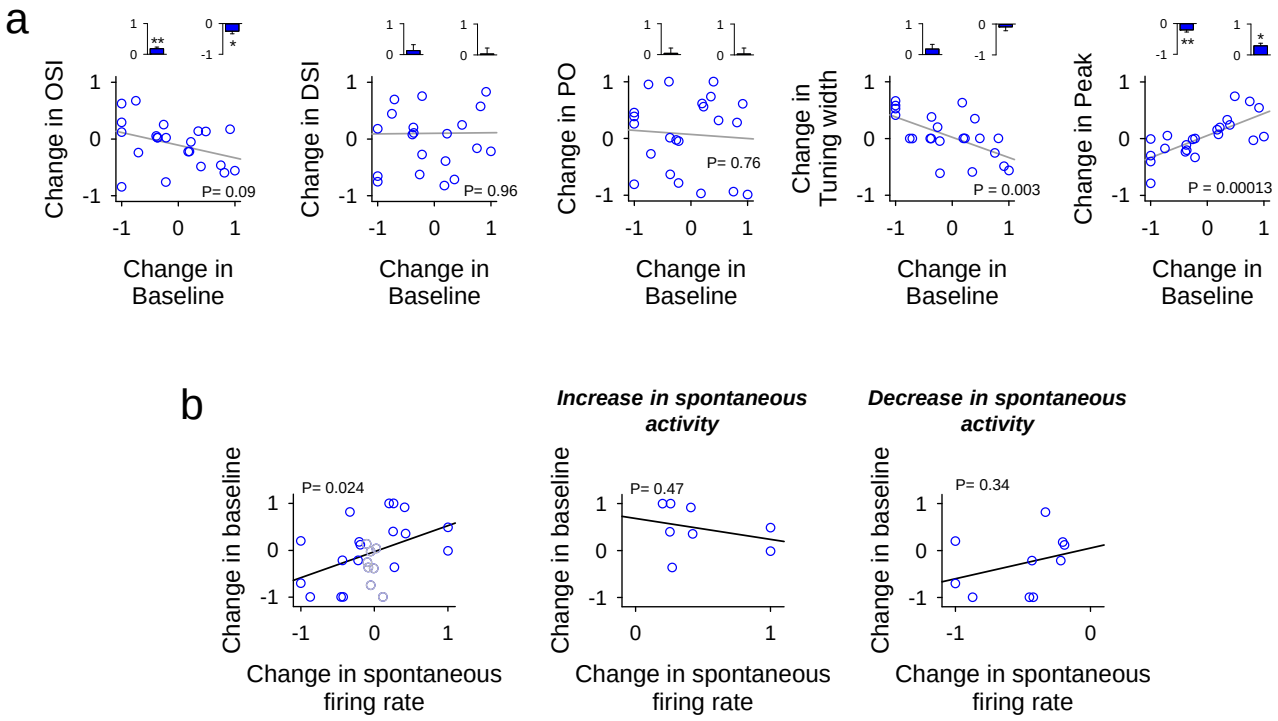


**Supplementary Figure 7. Astrocyte-induced changes in tuning parameters of SOM⁺ neurons.** (**a**) Normalized index of tuning parameters showing changes in OSI, DSI, preferred orientation, tuning width and peak amplitude vs baseline for SOM⁺ neurons. *Inset*: Normalized index for each parameter showing the differences before and after astrocyte stimulation (from Fig. 8e,g). *Inset Left*, normalized index for cells that showed decreases in the baseline after astrocyte stimulation. *Inset Right*, normalized index for cells that showed increases in the baseline after astrocyte stimulation. Circle, individual cell. Dashed line, linear regression for the population. (**b**) *Left,* Normalized index of firing rate showing changes in spontaneous firing rate vs baseline (visual-evoked firing rate) for SOM⁺ neurons. *Center-right,* Cells were classified according to significant changes in spontaneous firing rate, and are shown in these panels under *Increase in spontaneous activity* and *Decrease in spontaneous activity.* Circle, individual cell. Dashed line, linear regression for the population. Grey circles denote cells with no significant changes in spontaneous firing rate. SOM⁺ cells showed positive correlation between changes in baseline and specific response parameters.